Environmental Mercury Chemistry – In Silico

Abu Asaduzzaman,[1,2] Demian Riccardi,[3,4] Akef T. Afaneh,[1,5] Sarah J. Cooper,[6] Jeremy C. Smith,[3,4] Feiyue Wang,[7] Jerry M. Parks,[3,6] and Georg Schreckenbach[1*]

1 Department of Chemistry, University of Manitoba, Winnipeg, MB, Canada, R3T 2N2
2 School of Science, Engineering and Technology, Penn State Harrisburg, 777 West Harrisburg Pike, Middletown, PA 17057, USA
3 University of Tennessee/Oak Ridge National Laboratory Center for Molecular Biophysics, Biosciences Division, Oak Ridge National Laboratory, 1 Bethel Valley Road, Oak Ridge, TN 37831-6309, USA
4 Department of Biochemistry and Cellular and Molecular Biology, University of Tennessee Knoxville, Knoxville, Tennessee 37996, USA
5 Department of Chemistry, Faculty of Science, Al-Balqa Applied University, P. O. Box 19117, postal code 19117, Al-Salt, Jordan
6 Graduate School of Genome Science and Technology, University of Tennessee, Knoxville, Tennessee 37996, USA
7 Centre for Earth Observation Science and Department of Environment and Geography, University of Manitoba, Winnipeg, MB, Canada, R3T 2N2

*schrecke@cc.umanitoba.ca

Conspectus (Abstract)

Mercury (Hg) is a global environmental contaminant. Major anthropogenic sources of Hg emission include gold mining and the burning of fossil fuels. Once deposited in aquatic environments, Hg can undergo redox reactions, form complexes with ligands and adsorb onto particles. It can also be methylated by microorganisms. Mercury, especially its methylated form methylmercury, can be taken up by organisms, where it bioaccumulates and biomagnifies in the food chain, leading to detrimental effects on ecosystem and human health. In support of the recently enforced Minamata Convention on Mercury, a legally binding international convention aimed at reducing the anthropogenic emission of – and human exposure to – Hg, its global biogeochemical cycle must be understood. Thus, a detailed understanding of the molecular-level interactions of Hg is crucial.

The ongoing rapid development of hardware and methods has brought computational chemistry to a point that it can usefully inform environmental science. This is particularly true for Hg, which is difficult to handle experimentally due to its ultra-trace concentrations in the environment and its toxicity. The current account provides a synopsis of the application of computational chemistry to filling several major knowledge gaps in environmental Hg chemistry that have not been adequately addressed experimentally.

Environmental Hg chemistry requires defining the factors that determine the relative affinities of different ligands for Hg species, as they are critical for understanding its speciation, transformation and bioaccumulation in the environment. Formation constants and the nature of bonding have been determined computationally for environmentally relevant Hg(II) complexes such as chlorides, hydroxides, sulfides and selenides, in various physical phases. Quantum chemistry has been used to determine the driving forces behind the speciation of Hg with hydrochalcogenide and halide ligands. Of particular importance is the detailed characterization of

solvation effects. Indeed, the aqueous phase reverses trends in affinities found computationally in the gas phase. Computation has also been used to investigate complexes of methylmercury with (seleno)amino acids, providing a molecular-level understanding of the toxicological antagonism between Hg and selenium (Se). Furthermore, evidence is emerging that ice surfaces play an important role in Hg transport and transformation in polar and alpine regions. Therefore, the diffusion of Hg and its ions through an idealized ice surface has been characterized.

Microorganisms are major players in environmental mercury cycling. Some methylate inorganic Hg species, whereas others demethylate methylmercury. Quantum chemistry has been used to investigate catalytic mechanisms of enzymatic Hg methylation and demethylation. The complex interplay between the myriad chemical reactions and transport properties both in and outside microbial cells determines net biogeochemical cycling. Prospects for scaling up molecular work to obtain a mechanistic understanding of Hg cycling with comprehensive multi-scale biogeochemical modeling are also discussed.

Biographical Information

Abu Asaduzzaman is an Assistant Professor of Chemistry at Penn State Harrisburg. He obtained his Ph.D. from Saarland University.

Demian Riccardi is a Chemist in the Thermodynamics Research Center at the National Institute of Standards and Technology in Boulder, Colorado. He received his Ph.D. from the University of Wisconsin, Madison.

Akef T. Afaneh is an Assistant Professor of Physical Chemistry at Al-Balqa Applied University. He obtained his Ph.D. from the University of Manitoba.

Sarah J. Cooper is a graduate student in the Genome Science and Technology program at the University of Tennessee in Knoxville, Tennessee.

Jeremy C. Smith is a Governor's Chair at the University of Tennessee (UT) and Director of the UT/ORNL Center for Molecular Biophysics. He obtained his Ph.D. from the University of London.

Feiyue Wang is a Professor and Canada Research Chair in Arctic Environmental Chemistry at the University of Manitoba. He received his Ph.D. from Peking University.

Jerry M. Parks is an R&D Staff Scientist in the Biosciences Division at Oak Ridge National Laboratory. He received his Ph.D. from Duke University.

Georg Schreckenbach is a Professor of Chemistry at the University of Manitoba. He received his Ph.D. from the University of Calgary.

1. Introduction

Mercury (Hg) exists in nature largely as elemental Hg^0 (a liquid or monoatomic vapor) or its oxidized form, mercuric ion (Hg^{2+}), with the two forms undergoing interconversion through biotic and abiotic redox processes. Although trace amounts of mercurous ion, Hg^+, may be present in the environment, it is an unstable intermediate and tends to disproportionate rapidly to Hg^{2+} and Hg^0. Different Hg-containing species have markedly different chemical properties, bioavailabilities and toxicities. Unlike Hg^0, Hg^{2+} is highly reactive, nephrotoxic, hepatotoxic and immunotoxic.[1] Hg^{2+} is the most immediate substrate for the microbial formation of monomethylmercury, or simply methylmercury (CH_3Hg^+).[1] Methylmercury is transported across the blood-brain barrier and hence is neurotoxic. As methylmercury biomagnifies along the aquatic

food chain, consumption of predatory fish and other seafood is the major exposure pathway in humans.[1]

Consequently, a legally binding, international treaty, the Minamata Convention on Mercury, has recently entered into force to reduce anthropogenic emissions of Hg.[2] However, re-emissions of previously emitted Hg and its natural release from volcanoes and deep-sea vents will continue to impact terrestrial and marine biota. Thus, in support of the Minamata Convention, the global biogeochemical cycle of Hg must be understood, which requires a detailed understanding of the molecular-level interactions of Hg.

The ultra-trace concentrations of Hg in the environment (e.g., pM levels in natural waters) and the complexity and diversity of its chemical speciation are such that experimental characterization alone is unlikely to provide a complete description in the foreseeable future. Fortunately, the continued rapid development of computational modeling in general (hardware, software, and computational methods), and Hg chemistry in particular, has reached the point that it can usefully inform environmental science and augment, or even replace, difficult experimental investigations. This Account provides an overview of contributions toward filling key knowledge gaps in the global Hg cycle through the application of computational, i.e.*, in silico*, approaches.

2. Global Hg Cycle

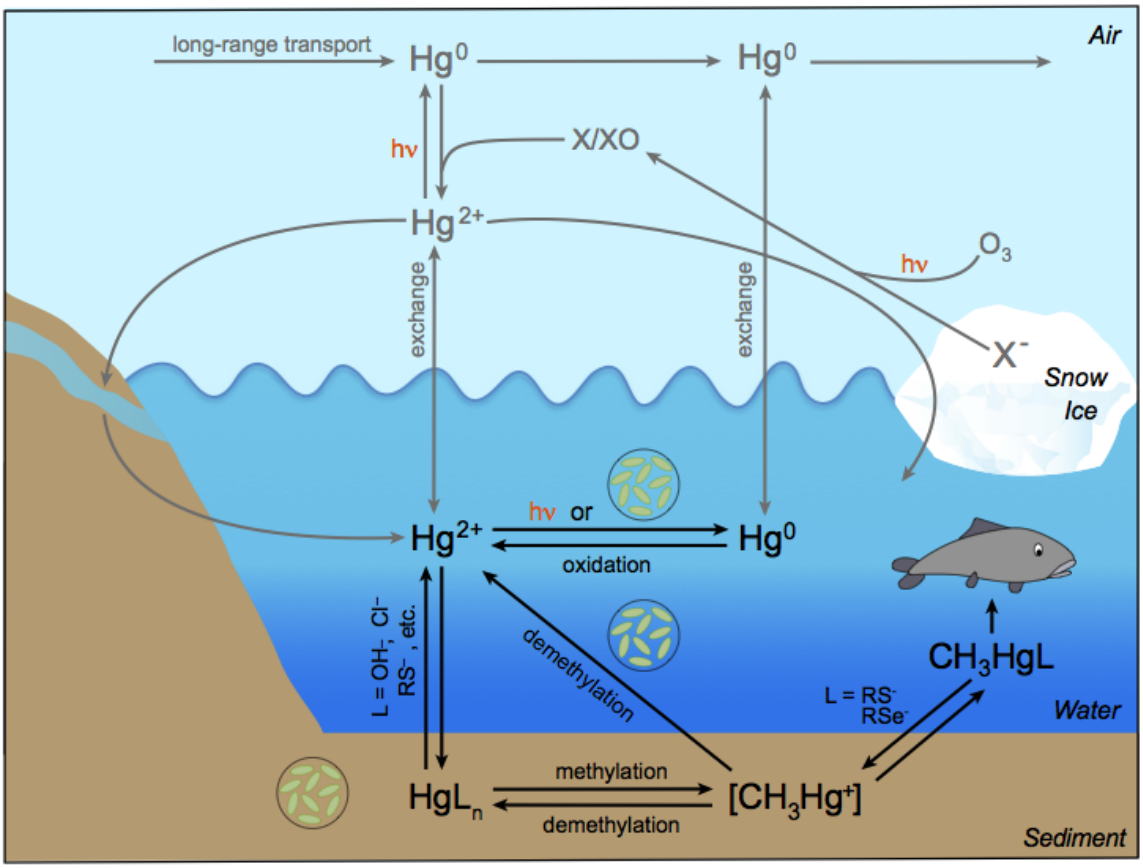

Figure 1. Selected transport and transformation processes in the global Hg cycle. hν: sunlight; X^-: halides; X/XO: halogen atoms and oxides; L: ligands that bind Hg^{2+} or CH_3Hg^+; RS^-/RSe^-: organic sulfides/selenides.

Global biogeochemical cycling of Hg (**Figure 1**) has been the subject of several recent reviews,[1,3,4] and therefore is only briefly summarized here. Currently, about (5.5–8.9) × 10^6 kg/yr of Hg are emitted into the atmosphere globally, about 10% of which is from primary natural sources (e.g., natural weathering of rocks, volcanic and geothermal activities), 30% from primary anthropogenic sources (including unintentional sectors such as coal burning, and intentional sectors such as artisanal and small-scale gold mining), and 60% from secondary (natural or anthropogenic) sources (i.e., re-emission of Hg previously deposited into the surface environment

from past natural or anthropogenic emissions).[5] The majority of atmospheric Hg is present as Hg^0, which has a sufficiently long lifetime (0.4−1.7 years[6,7]) in the global troposphere to allow its long-range transport to even the most remote regions, such as the Arctic and Antarctic. High Hg content in marine mammals in the Arctic Ocean has raised health concerns for Northern people and mammals.

Oxidation of Hg^0 to Hg^{2+} by a variety of oxidants is the primary mechanism for transferring atmospheric Hg^0 to the marine or terrestrial environments, as the resulting Hg^{2+} is readily scavenged by precipitation or atmospheric particles. In marine and terrestrial environments, Hg is present primarily as Hg^{2+} complexes with inorganic or organic nucleophilic ligands. Hg speciation is typically dominated by complexes with dissolved or colloidal organic matter and OH^- in fresh waters, and with Cl^- in seawater. However, in the presence of even trace amounts (pM to nM) of reduced sulfur compounds, such as in sediments, anoxic marine environments, and biological tissues, Hg speciation is dominated by its complexes with sulfide (SH^-), polysulfides (S_n^{2-}), or thiolate (RS^-) ligands; Hg(II) sulfide collects to form cinnabar, an ore that is used to refine elemental Hg.

Although Hg methylation can occur abiotically, in terrestrial and aquatic environments it is primarily mediated by microbial activity.[1] Demethylation of methylmercury and reduction of Hg^{2+} also occur in the terrestrial or aquatic environment, both of which are mediated photolytically or microbially. The resulting Hg^0 is then re-emitted back into the environment, closing the Hg cycle.

Computational methods have also been used to shed light on gaseous-phase reactions of Hg in the atmosphere, including both the oxidation of Hg^0 to Hg^{2+} (e.g., refs [8-10]) and the reduction of Hg^{2+} to Hg^0,[11] which are beyond the scope of this account. In the following sections we describe

computational methods used and then trace the path of Hg as it traverses through the aquatic environment.

3. Computational Methods

The quantum-mechanical method of choice is most often density functional theory (DFT), although some systems require the use of correlated (post-Hartree-Fock) levels of theory such as MP2, CASSCF or CCSD(T).[11] Relativistic effects must be included for a proper description of the chemistry of heavy elements such as Hg.[12] For instance, the radial velocity of a 1s electron in a hydrogen-like Hg^{79+} ion (Bohr model) is ~58% of the speed of light,[13] which leads to substantial contraction of that orbital (and other s and $p_{1/2}$ orbitals, due to the presence of the inner nodes, resulting in very large kinetic and potential energy contributions[14]). Higher angular momentum orbitals (d, f) are correspondingly expanded, due to the more effective screening of the nuclear charge.[15] Relativity even explains why Hg is a liquid at room temperature.[16]

Relativistic effects can be treated by various well-understood approaches of varying levels of theoretical rigor such as effective core potentials (ECP), the zeroth order relativistic approximation (ZORA), the Douglas-Kroll-Hess approximation, or the full four-component Dirac equation. Most often, these are applied in a scalar approximation. However, it can be important not to neglect spin-orbit effects, which split the energies of shells with non-zero angular momentum. An interesting example of the role of spin-orbit effects in Hg methylation has been published recently.[17] We have found that the different relativistic methods mentioned above can be used essentially interchangeably, when applied to valence properties such as geometries and energetics. Hence, the choice is often determined by practical considerations, e.g., speed or availability in a given code.

4. Hg Diffusion into Ice

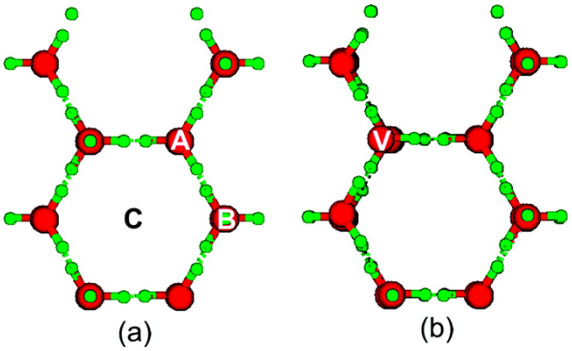

Figure 2. Top view of the optimized ice Ih surface for (**a**) stoichiometric and (**b**) defective surfaces. V denotes the position of the defect. Adsorption sites: **A** (on top of an O atom), **B** (on top of a H atom), and **c** (at the center of the hexagon). Reproduced with permission from ref. [18]. Copyright 2010 American Chemical Society.

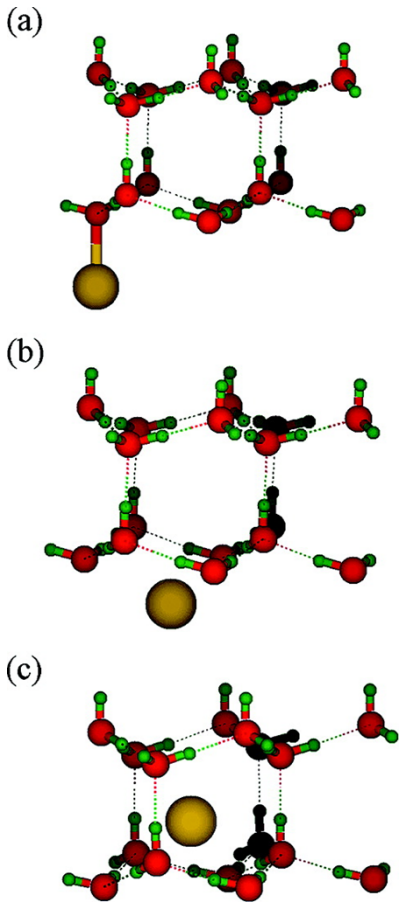

Figure 3. Local adsorption and interstitial sites for Hg on ice. (**a**,**b**) Sites A and B, respectively. (**c**) Interstitial site. Reproduced with permission from ref. [19]. Copyright 2012 American Chemical Society.

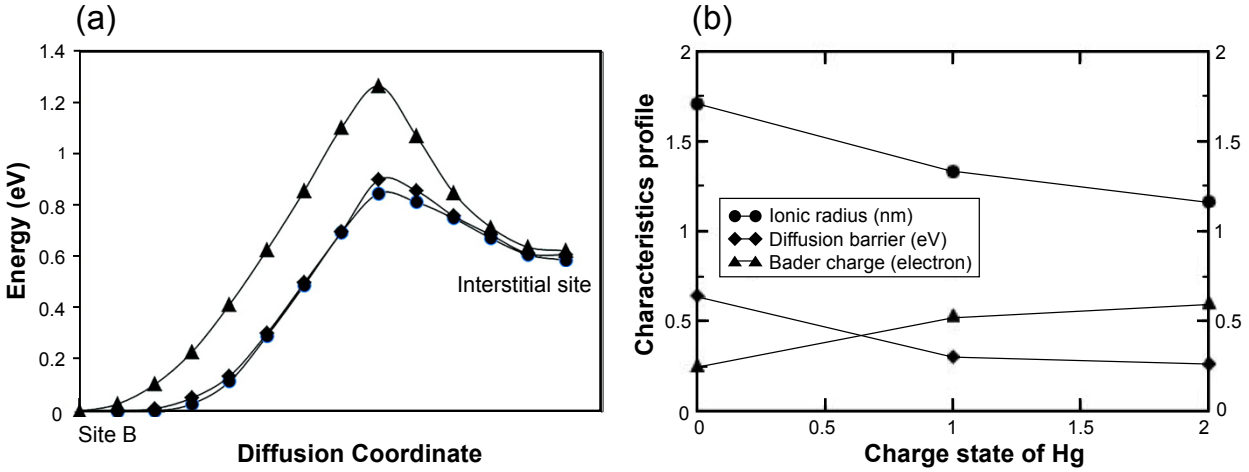

Figure 4. (**a**) Diffusion barrier from adsorption site B to the interstitial site for Hg^0 (▲), Hg^+ (◆), and Hg^{2+} (●). The energy for site B was set to zero for all species. (**b**) Variation of ionic radius (nm), diffusion barrier (eV), and Bader charge (in electrons) with the charge state of Hg. Reproduced with permission from ref. [19]. Copyright 2012 American Chemical Society.

Atmospheric Hg^0 is depleted in the spring through photochemical oxidation, thereby increasing surface concentrations of Hg^{2+}. However, a major question is how surface Hg in various oxidation states passes through a thick layer of ice to reach the water below, where it is eventually consumed by Arctic mammals. Although brine channels have been implicated as the primary transport mechanism,[20] diffusion is another fundamental mechanism for migration through ice layers. The atomic-scale mechanistic details of Hg diffusion in ice have been explored computationally.[19] Among the various phases of ice, Ih is the most prevalent under ambient conditions. Thus, we modeled an ideal ice(Ih) surface consisting of five layers as a model to

estimate the rates of diffusion of Hg^{m+}, where m = 0–2. Periodic plane-wave DFT was used with 2x2 supercells including appropriate vacuum space. To model charged species, Cl^- counterions were placed on the opposite site of the slab.

The first step of the diffusion process is adsorption. Thus, we calculated surface (**Figure 2**) and interstitial (**Figure 3**) adsorption sites[18] for Hg^{m+}, m = 0-2, for both ideal and defect ice surfaces. The adsorption energy varies depending on environment, becoming more favorable as the number of O donors interacting with Hg increases. We then used constrained minimization along the corresponding reaction coordinate compute diffusion pathways through bulk ice.[19] We found that the diffusion barrier of Hg into bulk ice (**Figure 4a**) depends on the charge state of Hg (**Figure 4b**). More highly charged Hg species have smaller ionic radii, which leads to lower diffusion barriers. Thus, Hg^{2+} diffuses through ice more rapidly than Hg(0), providing a plausible pathway from ice to the water below. Of course, Hg can also enter water through direct deposition or stream runoff (**Figure 1**).

5. Hg in Aqueous Solution

Central to understanding Hg cycling is the quantitative determination of the physicochemical factors that govern the behavior of Hg in aqueous systems. Thus, a detailed understanding of how Hg^{2+} ions and its potential ligands are hydrated is a prerequisite. In principle, solvation effects can be described computationally by continuum models, in which the solute molecule is embedded in a cavity within a polarizable dielectric medium[21] However, the solvation of ionic species remains a computational challenge because the bonding of solvent molecules in the local coordinating environment may be strong, anisotropic and specific, and these interactions are often not well described by continuum methods. To improve accuracy, a cluster comprising the solute and explicit solvent molecules can be constructed and immersed in a dielectric

continuum.[22-25]

We developed a cluster-continuum approach to compute the standard state aqueous solvation free energies (ΔG^*_s) of Cu^{2+}, group 12 metal cations (Zn^{2+}, Cd^{2+}, Hg^{2+}) and the anions OH^-, SH^-, Cl^-, and F^-,[26] using a thermodynamic cycle that includes small clusters of a few explicit water molecules.[25] Analysis of the trends within each set revealed good agreement with experiment, although, as is often the case with quantum chemistry, this is due in part to error cancellation. The standard deviation of ΔG^*_s was ~1 kcal/mol for both metal cations and anions clustered with 10 and 8 water molecules, respectively, and 2.3 kcal/mol for the entire set of eight ions. The relative trends of ions with the same charge were dominated by local interactions with the solvent. This study provided a foundation upon which Hg complexation and speciation could then be examined.

6. Hg-ligand complexation

We extended the cluster-continuum approach to compute aqueous ligand binding free energies ($\Delta G^*_{bind,aq}$) for Hg^{2+} with a small set of inorganic (hydrochalogenide and halide) ligands.[27] Accurate relative ligand binding free energies were obtained with only a few explicit waters (i.e., n=6 for Hg^{2+} and n=2 for anionic ligands). For the relative binding free energy difference, $\Delta\Delta G^*_{bind,aq}$, we obtained a mean signed error of 0.7 kcal/mol. This approach reproduced the experimentally observed trend in binding free energies: $Hg(SH)_2 > Hg(OH)_2 > HgBr_2 \approx Hg(OH)Cl > HgCl_2$.

Hg-ligand binding free energies were then examined as a function of the number of solvating water molecules, ranging from gas-phase (no water molecules, $\Delta\Delta G^\circ_{bind,g}$) to the full cluster-continuum model. Interestingly, the gas-phase interaction of Hg^{2+} with $2OH^-$ ligands is much stronger (by 30.5 kcal/mol) than that with $2SH^-$. However, upon adding only two gas-phase

solvating water molecules for each species (i.e., the relative solvation free energy, $\Delta\Delta G^*_s$, without continuum contributions) the binding of $2SH^-$ is favored by 7 kcal/mol. This large energetic shift results from the difference in the strength of interaction between anions and water. In bulk water, $Hg(SH)_2$ is favored over $Hg(OH)_2$ by -22.8 kcal/mol. The switch in preferred ligand is driven largely by the difference of 65.2 kcal/mol between the solvation free energies of $2SH^-$ and $2OH^-$. OH^- ions are much more sequestered by solvent than SH^-, which may at least partly be a function of size.[28] Thus, the preference of Hg^{2+} for soft ligands such as thiols is determined by local solvation effects. These effects also describe periodic trends for chalcogenide and halide ligands.

In parallel, a cluster-continuum method was used to predict the formation constant (K) of the neutral aqueous complex HgS.[29] The K values for HgS (for the reaction of $Hg^{2+} + HS^- = HgS + H^+$) previously estimated from a simple linear free energy relationship differ by twelve orders of magnitude (i.e., from $10^{14.2}$ to $10^{26.5}$).[30] After successfully reproducing the experimental K values for a set of aqueous Hg(II) complexes, these calculations yielded an estimated K value of $10^{27.2}$ for HgS, which is close to the high end of the previously estimated range.[30] It should be noted, however, that a recent experimental study has ruled out the significance of HgS under low sulfide concentrations.[31]

7. Calculation of ligand pK_as and Hg-ligand stability constants

Mixed cluster-continuum approaches provide good accuracy for Hg complexes, but these calculations are computationally demanding because they require thorough conformational searches to identify low-energy minima. For Hg complexes with larger ligands such as those found in dissolved organic matter (DOM), including an appropriate number of explicit water molecules can be prohibitive. Thus, we developed an approach to calculating accurate thermodynamic quantities with a modified continuum model that does not require explicit water.

Hg^{2+} competes with H^+ for metal-binding functional groups, such as carboxylic acids, amines, and, in particular, thiols. Thus, Hg speciation is intimately related to the pK_as of organic ligands. Calculating pK_as of thiols with DFT and a standard continuum solvent model yields errors of up to 10 pK units, due mainly to inaccuracies in the solvation free energies of thiolates. Application of the scaled solvent-accessible surface approach resulted in mean unsigned errors of 0.9, 0.4, and 0.5 pK units, respectively, for a set of carboxylic acids, aliphatic amines, and thiols.[32] We then extended this approach to enable calculation of log K values. For a set of environmentally relevant Hg complexes, we obtained a mean unsigned error of ~1.6 log units compared to experimental values.[33]

Hg interacts strongly with dissolved organic matter (DOM). However, the extreme heterogeneity of DOM makes the identification of specific Hg-DOM complexes quite challenging. By combining ultrahigh-resolution mass spectrometry, which provides highly accurate chemical formulas, with DFT calculations of log β for putative molecular structures, we identified Hg(II) bis(N,N-diethyldithiolate) as a specific constituent of Hg-DOM.[34] The quantum chemical approaches we have developed are therefore useful for efficiently calculating pK_as and stability constants for environmentally relevant species and identifying specific constituents of complex environmental samples.

8. Transformation of Hg by microorganisms

Microorganisms are highly influential in Hg speciation and transformation. They are major players in Hg redox reactions and the formation and degradation of toxic methylmercury. Therefore, microorganisms play key roles in the global biogeochemical cycling of Hg (**Figure 1**).

8.1 Bacterial Hg methylation

Some anaerobic microorganisms convert inorganic Hg species to methylmercury. Recently, a combination of chemical reasoning, comparative genomics, and 3D protein modeling led to the discovery of the genes *hgcA* and *hgcB*, which confer the ability to methylate Hg.[35]

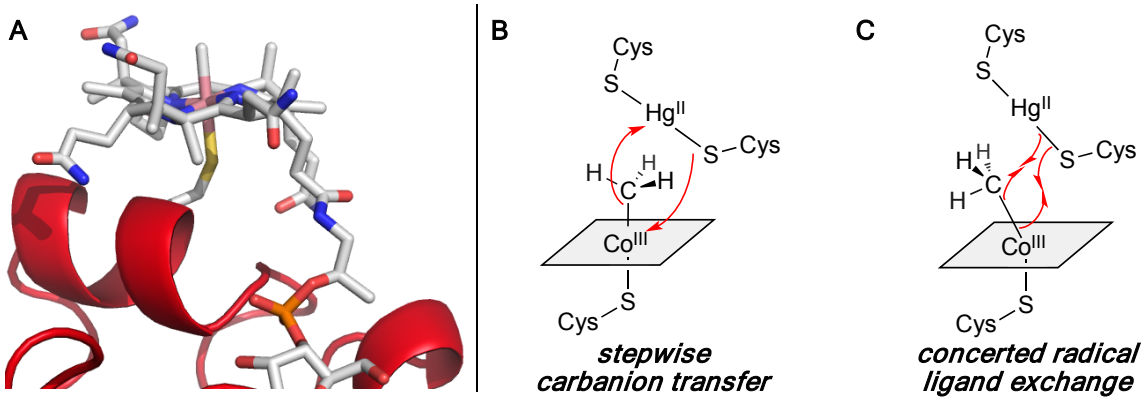

Figure 5. (**A**) Homology model of HgcA. Proposed mechanisms for Hg methylation. Adapted with permission from ref. 35. Copyright 2013 American Association for the Advancement of Science. (**B**) carbanion transfer and (**C**) concerted radical ligand exchange. Adapted with permission from ref. 36. Copyright 2014 American Chemical Society.

Homology modeling of the corrinoid-binding domain of HgcA revealed that a strictly conserved Cys in HgcA is likely coordinated to the Co center in vitamin B12 (**Figure 5A**), a feature that had not been observed previously for any corrinoid protein. We proposed that this Cys ligand to Co plays a major role in facilitating methyl transfer to Hg(II). We then generated a quantum chemical cluster model of HgcA and used DFT with a scalar relativistic ECP to calculate reaction free energies for methyl transfer as either a methyl carbanion or methyl radical (**Figure 5B**).[36] We found that the carbanion pathway was thermodynamically more favorable. On the basis of our calculations, we predicted that substitution of Cys with His might also afford the production of methylmercury, but substitution with Ala would abolish its formation completely. Those

predictions were confirmed through in vivo site-directed mutagenesis experiments,[37] demonstrating the predictive power of the DFT models. However, a subsequent DFT study performed with a spin-orbit ZORA approach found that the radical-based ligand exchange mechanism (**Figure 5B**) is energetically more favorable than the carbanion pathway, but only when spin-orbit effects are included.[17] Thus, spin-orbit effects appear to make an important contribution to catalysis in Hg methylation by HgcA.

8.2 Bacterial Hg Resistance

Certain bacteria carry a suite of co-transcribed genes, called the Hg resistance (*mer*) operon, whose protein products convert methylmercury and Hg^{2+} compounds to less toxic forms.[38] The enzyme organomercurial lyase (MerB) cleaves the Hg–C bond in methylmercury, and mercuric reductase (MerA) reduces Hg^{2+} to Hg^0.

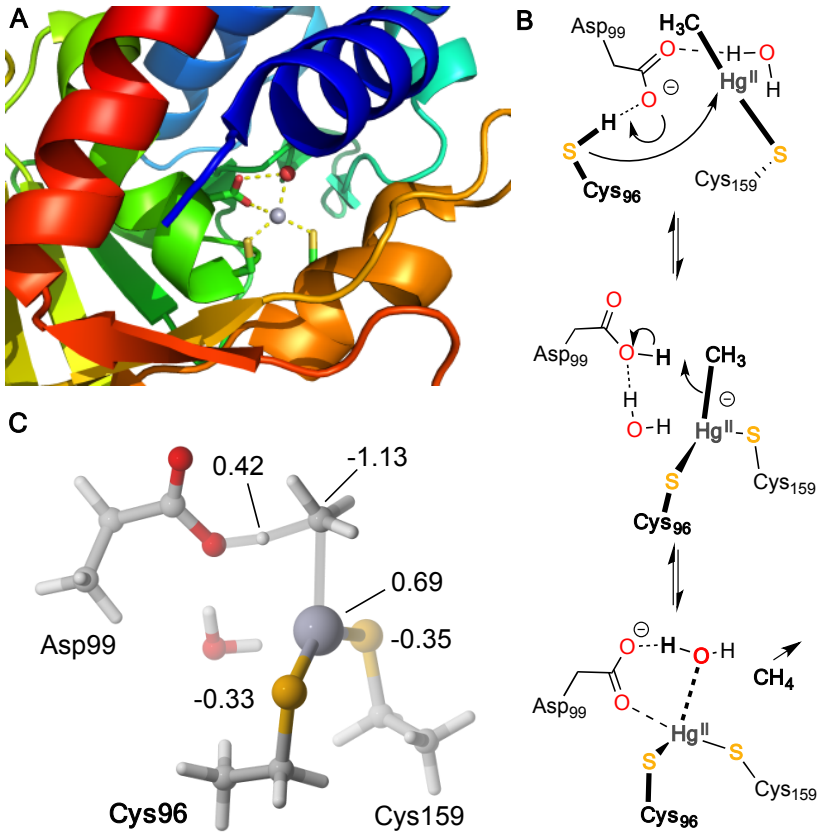

Figure 6. (**A**) X-ray crystal structure of MerB,[39] **B**) Proposed mechanism for the Hg–C cleavage reaction catalyzed by the organomercurial lyase, MerB, (**C**) Quantum chemical cluster model of the rate-limiting transition state for the Hg–C cleavage reaction. Partial charges for selected atoms are labeled. Adapted with permission from ref. 41. Copyright 2009 American Chemical Society.

The active site of MerB contains two Cys and one Asp residue (**Figure 6**), all of which are required for activity.[40] We used hybrid DFT with a scalar ECP to characterize the mechanism of Hg–C bond cleavage in an active site model of MerB.[41] Coordination of methylmercury by both Cys residues forms a trigonal intermediate. The catalytic Asp then protonates the methyl group in methylmercury to liberate CH_4, with Hg^{2+} remaining coordinated to the two Cys residues. Computed energy barriers for three organomercurial substrates were all within ~1 kcal/mol of experimentally determined activation free energies derived from k_{cat} measurements.[40] Partial charges obtained from natural population analysis[42] of the computed transition state revealed an increase in electron density on the forming carbanion, as well as an elongation of the Hg–C bond, both of which result from the *bis* coordination of CH_3Hg^+ by the two cysteines (**Figure 6**). These findings showed how Hg-resistant bacteria detoxify methylmercury.

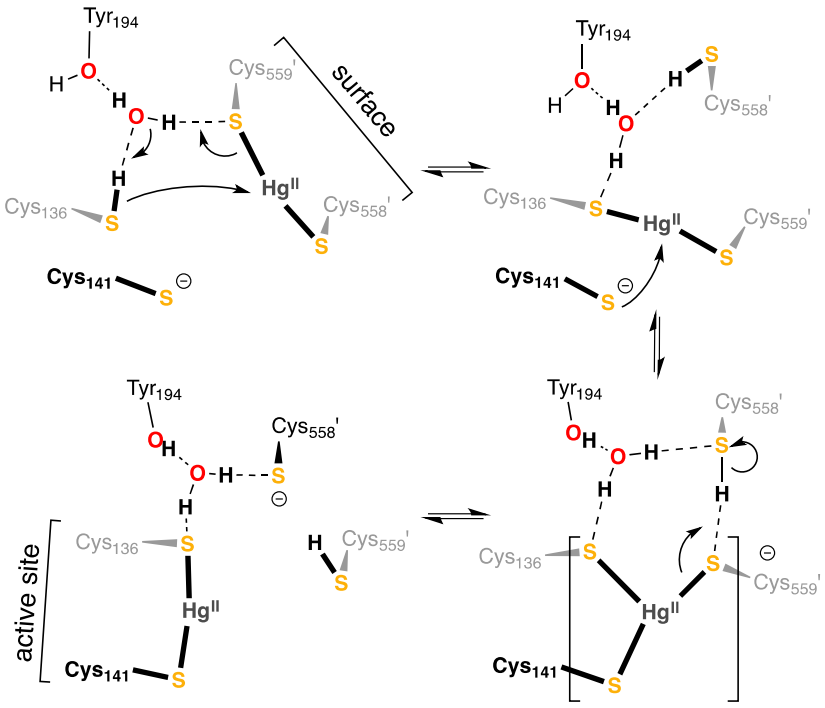

Figure 7. Proposed mechanism for intramolecular Hg(II) transfer from the outer pair of Cys residues (Cys558' and Cys559') to the inner pair (Cys136 and Cys141) in MerA. Adapted with permission from ref. 46. Copyright 2014 American Chemical Society.

MerA is an NADPH-dependent flavoenzyme that catalyzes the reduction of Hg^{2+} to Hg^0. MerA obtains Hg^{2+} from various sources, including the active site of MerB. MerA proteins often include two metallochaperone domains, NmerA, which acquire Hg^{2+} and deliver it the catalytic core domain for reduction.[43,44] Upon binding to a surface-exposed pair of Cys residues, Hg^{2+} is transferred to another pair of Cys residues in the active site of MerA. Using QM/MM,[45] which enables reactions to be modeled in a complete enzyme-solvent system, we calculated structures and energies for a multi-step pathway in which Hg^{2+} is transferred from the outer to the inner Cys pair prior to being reduced to Hg^0 (**Figure 7**).[46] A general feature of the proteins and enzymes of the *mer* operon was found to be the use of pairs of Cys residues and acid/base chemistry to bind

Hg^{2+} with high affinity and orchestrate intra- and intermolecular transfers and transformations. Once Hg^{2+} is reduced in a subsequent step, Hg^0 diffuses out of the cell, where it continues its perpetual cycle in the environment.

9. (Seleno)amino Acid Complexes

Se imparts a protective effect against Hg bioaccumulation, but the reasons are not well understood.[47] Because of their similar chemical properties, Se can replace S in amino acids. Is this feature responsible for the Hg–Se antagonism? To address this question, methylmercury complexes of four seleno-amino acids,[48] cysteine, methionine, glutathione and penicillamine, were synthesized and characterized in comparison to their S counterparts, using both experimental and computational techniques.[48,49]

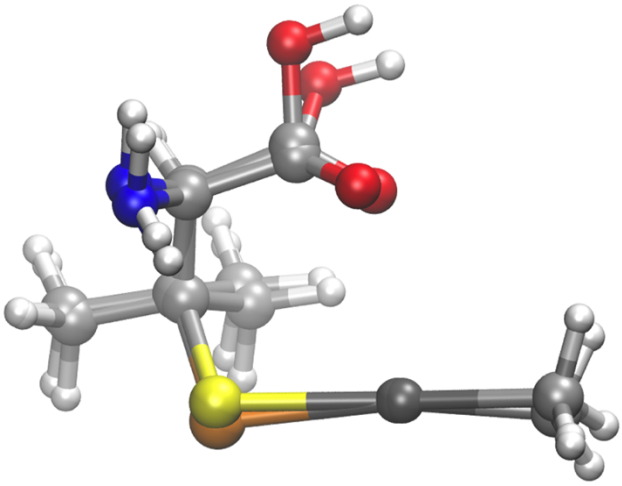

Figure 8. Superimposed optimized structures of MeHg-D,L-penicillamine and MeHg-D,L-selenopenicillamine. *Colors*: H, white; C, light gray; N, blue; O, red; S, yellow; Se, orange; Hg, dark gray. Adapted with permission from ref. [49]. Copyright 2010 American Chemical Society.

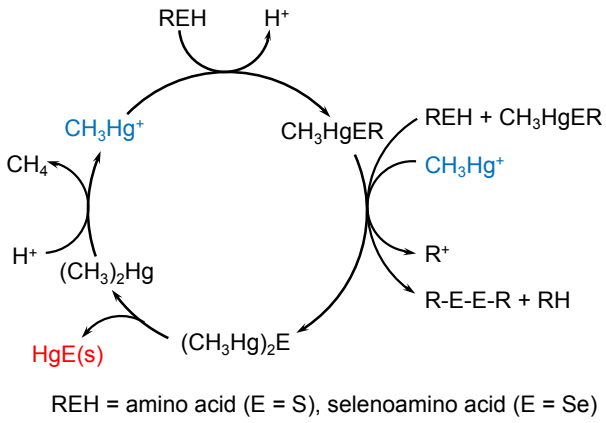

Figure 9. Proposed mechanism for in vivo formation of HgE(s), E = S, Se. Reproduced with permission from ref. [50]. Copyright 2010 American Chemical Society.

Complexes between methylmercury and amino acids have very similar geometries compared to the corresponding selenoamino acid complexes, with slight differences related to the difference in size between S and Se (**Figure 8**).[48,49] Likewise, the electronic structures are similar, with subtle differences in HOMO-LUMO gaps and slightly greater covalency for the Se complexes (Table S1). These differences result in generally lower stability of the Se complexes, including weaker Hg–E and C–E bonds (E = S, Se). For instance, the reaction energy difference for reaction (1) shows that the Hg–Se bond is 2.7 kcal/mol weaker than its Hg–S counterpart:

$$CH_3Hg–Cys \rightarrow CH_3Hg^+ + Cys(–) \quad (1)$$

Neutral fragments on the right-hand side of Eq. (1) gave similar differences between Hg–S and Hg–Se bond strengths, as did calculations for other systems containing Hg–E bonds[49] including small, binary HgE and large, bulky complexes, as has been shown in a detailed study of the *chalcogenophilicity* of Hg.[51] To address the mechanism of toxicological antagonism,[47] we developed a model that captures the essence of the experiment (**Figure 9**):

$$CH_3HgOH + AH \rightarrow CH_3HgA + H_2O \quad (2)$$

where AH is a (seleno)amino acid. We found that the free energies of formation for the selenoamino acids are lower by 2 to 8 kcal/mol than for the corresponding amino acid complexes (**Table 1**). This thermodynamic favorability can be understood from the lower stability of the reactant selenoamino acids and may explain the toxicological Hg–Se antagonism.[49]

Table 1. Calculated reaction free energies in solution for reaction (2)[a]

Reagent AH	ΔG_r (kcal/mol)
cysteine	-16.8
selenocysteine	-19.0
penicillamine	-12.1
selenopenicillamine	-19.9
gluthathione	-14.6
selenogluthathione	-18.8
methionine[a,b]	6.7
selenomethionine[a,b]	2.3

(a) Ref. [49]. See SI for more detailed discussion.

(b) Model for high pH.

Once CH_3Hg–SeR complexes are formed in vivo, what is the mechanism for their degradation? This question was addressed both experimentally[52] and computationally.[50] A proposed mechanism is shown in **Figure 9**, the thermodynamics of which was probed computationally using (seleno)cysteine as representative amino acid.[50] A key result was that, while structures and general reactions are rather similar, all the Se-containing reactions are more

favorable than their S-counterparts. The thermodynamics therefore supports the Se–Hg antagonism.

10. Conclusions

Computational environmental Hg chemistry provides an excellent example of the breadth and reach of modern computational chemistry. Indeed, computational chemistry can now tackle some of the complexities inherent in experimental situations in general, and in environmental Hg chemistry in particular. This point has been illustrated in the present Account, which covers several parts of the Hg cycle (**Figure 1**), including diffusion through ice (**section 4**), aqueous systems (**sections 5**-**6**), microbial transformations (**section 8**), and Se–Hg antagonism (**section 9**).

A remaining challenge is how to implement the molecular scale approaches described here to scale up to much larger spatial scales, such as mesoscale thermodynamic speciation modeling and reach-to-watershed scale modeling. Although experimental thermodynamics databases involving Hg speciation exist,[53] substantial uncertainties remain in *K* values, kinetics and mechanisms of individual biotic and abiotic processes transforming Hg, including those in which the metal is oxidized, reduced, complexed, methylated or demethylated. Integration of the results into mesoscale models has the potential to improve the predictive power of reach-to-watershed scale Hg cycling with reactive transport modeling codes such as PFLOTRAN.[54]

Acknowledgments

Three research groups at two different institutions have come together for this account. Initially, we had corresponded about failure to cite each other's papers, but we decided to turn this experience around. The result is this account: "When handed a lemon, make lemonade!" GS and

FW acknowledge funding from NSERC, and FW from the Canada Research Chairs program. JP, DR and JS acknowledge support from the US Department of Energy (DOE), Office of Science, Office of Biological and Environmental Research, through the Mercury Scientific Focus Area at Oak Ridge National Laboratory (ORNL) and the Subsurface Biogeochemical Research (SBR) program at the University of Tennessee Knoxville and ORNL through Grants DE-SC0004895 and DE-SC0016478 from the US Department of Energy (DOE). ORNL is managed by UT-Battelle, LLC, for the US Department of Energy under contract DE-AC05-00OR22725. SJC was supported by NIH/NIGMS-IMSD Grant No. R25GM086761 and a National Science Foundation Graduate Research Fellowship under Grant No. 2017219379.

Supporting Information Available

Electronic properties of (seleno)amino acid-MeHg complexes (**Table S1**); extended version of **Table 1** (**Table S2**); accompanying discussion.

References

(1) Driscoll, C. T.; Mason, R. P.; Chan, H. M.; Jacob, D. J.; Pirrone, N.: Mercury as a Global Pollutant: Sources, Pathways, and Effects. *Environ. Sci. Technol.* **2013**, *47*, 4967-4983.
(2) http://www.mercuryconvention.org/, accessed 2018-11-22.
(3) Fitzgerald, W. F.; Lamborg, C. H.; Hammerschmidt, C. R.: Marine Biogeochemical Cycling of Mercury. *Chem. Rev.* **2007**, *107*, 641-662.
(4) Ariya, P. A.; Amyot, M.; Dastoor, A.; Deeds, D.; Feinberg, A.; Kos, G.; Poulain, A.; Ryjkov, A.; Semeniuk, K.; Subir, M.; Toyota, K.: Mercury Physicochemical and Biogeochemical Transformation in the Atmosphere and at Atmospheric Interfaces: A Review and Future Directions. *Chem. Rev.* **2015**, *115*, 3760-3802.
(5) UNEP "Global Mercury Assessment 2013. Sources, Emissions, Releases and Environmental Transport," Geneva, Switzerland, 2013.
(6) Holmes, C. D.; Jacob, D. J.; Yang, X.: Global lifetime of elemental mercury against oxidation by atomic bromine in the free troposphere. *Geophys. Res. Lett.* **2006**, *33*, L20808.
(7) Horowitz, H. M.; Jacob, D. J.; Zhang, Y. X.; Dibble, T. S.; Slemr, F.; Amos, H. M.; Schmidt, J. A.; Corbitt, E. S.; Marais, E. A.; Sunderland, E. M.: A new mechanism for atmospheric mercury redox chemistry: implications for the global mercury budget. *Atmos. Chem. Phys.* **2017**, *17*, 6353-6371.
(8) Dibble, T. S.; Zelie, M. J.; Mao, H.: Thermodynamics of reactions of ClHg and BrHg radicals with atmospherically abundant free radicals. *Atmos. Chem. Phys.* **2012**, *12*, 10271-10279.
(9) Goodsite, M. E.; Plane, J. M. C.; Skov, H.: A theoretical study of the oxidation of Hg-0 to HgBr2 in the troposphere. *Environ. Sci. Technol.* **2004**, *38*, 1772-1776.
(10) Goodsite, M. E.; Plane, J. M. C.; Skov, H.: A Theoretical Study of the Oxidation of Hg0 to HgBr2 in the Troposphere (vol 38, pg 1772, 2004). *Environ. Sci. Technol.* **2012**, *46*, 5262-5262.
(11) Saiz-Lopez, A.; Sitkiewicz, S. P.; Roca-Sanjuan, D.; Oliva-Enrich, J. M.; Davalos, J. Z.; Notario, R.; Jiskra, M.; Xu, Y.; Wang, F.; Thackray, C. P.; Sunderland, E. M.; Jacob, D. J.; Travnikov, O.; Cuevas, C. A.; Acuna, A. U.; Rivero, D.; Plane, J. M. C.; Kinnison, D. E.; Sonke, J. E.: Photoreduction of gaseous oxidized mercury changes global atmospheric mercury speciation, transport and deposition. *Nature Communications* **2018**, *9*, 4796.
(12) Pyykkö, P.: Relativistic Effects in Structural Chemistry. *Chem. Rev.* **1988**, *88*, 563-594.
(13) Thayer, J. S.: Relativistic effects and the chemistry of the heaviest main-group elements. *J. Chem. Educ.* **2005**, *82*, 1721-1727.
(14) Autschbach, J.: Perspective: Relativistic effects. *J. Chem. Phys.* **2012**, *136*, 150902.
(15) Schwarz, W. H. E.; van Wezenbeek, E. M.; Baerends, E. J.; Snijders, J. G.: The Origin of Relativistic Effects of Atomic Orbitals. *Journal of Physics B* **1989**, *22*, 1515-1530.
(16) Calvo, F.; Pahl, E.; Wormit, M.; Schwerdtfeger, P.: Evidence for Low-Temperature Melting of Mercury owing to Relativity. *Angew. Chem., Int. Ed.* **2013**, *52*, 7583-7585.
(17) Demissie, T. B.; Garabato, B. D.; Ruud, K.; Kozlowski, P. M.: Mercury Methylation by Cobalt Corrinoids: Relativistic Effects Dictate the Reaction Mechanism. *Angew. Chem., Int. Ed.* **2016**, *55*, 11503-11506.
(18) Asaduzzaman, A. M.; Schreckenbach, G.: Adsorption of Na and Hg on the Ice(Ih) Surface: A Density-Functional Study. *J. Phys. Chem. C* **2010**, *114*, 2941-2946.
(19) Asaduzzaman, A. M.; Wang, F. Y.; Schreckenbach, G.: Quantum-Chemical Study of the Diffusion of Hg(0, I, II) into the Ice(Ih). *J. Phys. Chem. C* **2012**, *116*, 5151-5154.

(20) Chaulk, A.; Stern, G. A.; Armstrong, D.; Barber, D. G.; Wang, F. Y.: Mercury Distribution and Transport Across the Ocean-Sea-Ice-Atmosphere Interface in the Arctic Ocean. *Environ. Sci. Technol.* **2011**, *45*, 1866-1872.
(21) Tomasi, J.; Mennucci, B.; Cammi, R.: Quantum Mechanical Continuum Solvation Models. *Chem. Rev.* **2005**, *105*, 2999-3093.
(22) Pliego, J. R.; Riveros, J. M.: The Cluster-Continuum Model for the Calculation of the Solvation Free Energy of Ionic Species. *J. Phys. Chem. A* **2001**, *105*, 7241-7247.
(23) Zhan, C. G.; Dixon, D. A.: Absolute hydration free energy of the proton from first-principles electronic structure calculations. *J. Phys. Chem. A* **2001**, *105*, 11534-11540.
(24) Rempe, S. B.; Pratt, L. R.; Hummer, G.; Kress, J. D.; Martin, R. L.; Redondo, A.: The Hydration Number of Li(+) in Liquid Water. *J. Am. Chem. Soc.* **2000**, *122*, 966-967.
(25) Bryantsev, V. S.; Diallo, M. S.; Goddard, W. A.: Calculation of solvation free energies of charged solutes using mixed cluster/continuum models. *J. Phys. Chem. B* **2008**, *112*, 9709-9719.
(26) Riccardi, D.; Guo, H. B.; Parks, J. M.; Gu, B. H.; Liang, L. Y.; Smith, J. C.: Cluster-Continuum Calculations of Hydration Free Energies of Anions and Group 12 Divalent Cations. *J. Chem. Theory Comput.* **2013**, *9*, 555-569.
(27) Riccardi, D.; Guo, H. B.; Parks, J. M.; Gu, B. H.; Summers, A. O.; Miller, S. M.; Liang, L. Y.; Smith, J. C.: Why Mercury Prefers Soft Ligands. *J. Phys. Chem. Lett.* **2013**, *4*, 2317-2322.
(28) Schreckenbach, G.: Differential Solvation. *Chem. Eur. J.* **2017**, *23*, 3797-3803.
(29) Afaneh, A. T.; Schreckenbach, G.; Wang, F. Y.: Theoretical Study of the Formation of Mercury (Hg2+) Complexes in Solution Using an Explicit Solvation Shell in Implicit Solvent Calculations. *J. Phys. Chem. B* **2014**, *118*, 11271-11283.
(30) Dyrssen, D.; Wedborg, M.: The Sulfur-Mercury(II) System in Natural-Waters. *Water Air and Soil Pollution* **1991**, *56*, 507-519.
(31) Drott, A.; Bjorn, E.; Bouchet, S.; Skyllberg, U.: Refining Thermodynamic Constants for Mercury(II)-Sulfides in Equilibrium with Metacinnabar at Sub-Micromolar Aqueous Sulfide Concentrations. *Environ. Sci. Technol.* **2013**, *47*, 4197-4203.
(32) Lian, P.; Johnston, R. C.; Parks, J. M.; Smith, J. C.: Quantum Chemical Calculation of pK(a)s of Environmentally Relevant Functional Groups: Carboxylic Acids, Amines, and Thiols in Aqueous Solution. *J. Phys. Chem. A* **2018**, *122*, 4366-4374.
(33) Devarajan, D.; Lian, P.; Brooks, S. C.; Parks, J. M.; Smith, J. C.: Quantum Chemical Approach for Calculating Stability Constants of Mercury Complexes. *ACS Earth and Space Chemistry* **2018**, *2*, 1168-1178.
(34) Chen, H.; Johnston, R. C.; Mann, B. F.; Chu, R. K.; Tolic, N.; Parks, J. M.; Gu, B.: Identification of Mercury and Dissolved Organic Matter Complexes Using Ultrahigh Resolution Mass Spectrometry. *Environmental Science & Technology Letters* **2017**, *4*, 59-65.
(35) Parks, J. M.; Johs, A.; Podar, M.; Bridou, R.; Hurt, R. A.; Smith, S. D.; Tomanicek, S. J.; Qian, Y.; Brown, S. D.; Brandt, C. C.; Palumbo, A. V.; Smith, J. C.; Wall, J. D.; Elias, D. A.; Liang, L. Y.: The Genetic Basis for Bacterial Mercury Methylation. *Science* **2013**, *339*, 1332-1335.
(36) Zhou, J.; Riccardi, D.; Beste, A.; Smith, J. C.; Parks, J. M.: Mercury Methylation by HgcA: Theory Supports Carbanion Transfer to Hg(II). *Inorg. Chem.* **2014**, *53*, 772-777.
(37) Smith, S. D.; Bridou, R.; Johs, A.; Parks, J. M.; Elias, D. A.; Hurt, R. A.; Brown, S. D.; Podar, M.; Wall, J. D.: Site-Directed Mutagenesis of HgcA and HgcB Reveals Amino Acid Residues Important for Mercury Methylation. *Appl. Environ. Microbiol.* **2015**, *81*, 3205-3217.

(38) Barkay, T.; Miller, S. M.; Summers, A. O.: Bacterial mercury resistance from atoms to ecosystems. *Fems Microbiology Reviews* **2003**, *27*, 355-384.
(39) Lafrance-Vanasse, J.; Lefebvre, M.; Di Lello, P.; Sygusch, J.; Omichinski, J. G.: Crystal Structures of the Organomercurial Lyase MerB in Its Free and Mercury-bound Forms: Insights Into the Mechanism of Methylmercury Degradation. *J. Biol. Chem.* **2009**, *284*, 938-944.
(40) Pitts, K. E.; Summers, A. O.: The roles of thiols in the bacterial organomercurial lyase (MerB). *Biochemistry* **2002**, *41*, 10287-10296.
(41) Parks, J. M.; Guo, H.; Momany, C.; Liang, L. Y.; Miller, S. M.; Summers, A. O.; Smith, J. C.: Mechanism of Hg-C Protonolysis in the Organomercurial Lyase MerB. *J. Am. Chem. Soc.* **2009**, *131*, 13278-13285.
(42) Reed, A. E.; Weinstock, R. B.; Weinhold, F.: Natural Population Analysis. *J. Chem. Phys.* **1985**, *83*, 735-746.
(43) Johs, A.; Harwood, I. M.; Parks, J. M.; Nauss, R. E.; Smith, J. C.; Liang, L. Y.; Miller, S. M.: Structural Characterization of Intramolecular Hg (2+) Transfer between Flexibly Linked Domains of Mercuric Ion Reductase. *J. Mol. Biol.* **2011**, *413*, 639-656.
(44) Hong, L.; Sharp, M. A.; Poblete, S.; Bieh, R.; Zamponi, M.; Szekely, N.; Appavou, M. S.; Winkler, R. G.; Nauss, R. E.; Johs, A.; Parks, J. M.; Yi, Z.; Cheng, X. L.; Liang, L. Y.; Ohl, M.; Miller, S. M.; Richter, D.; Gompper, G.; Smith, J. C.: Structure and Dynamics of a Compact State of a Multidomain Protein, the Mercuric Ion Reductase. *Biophys. J.* **2014**, *107*, 393-400.
(45) Senn, H. M.; Thiel, W.: QM/MM Methods for Biomolecular Systems. *Angew. Chem., Int. Ed.* **2009**, *48*, 1198-1229.
(46) Lian, P.; Guo, H. B.; Riccardi, D.; Dong, A. P.; Parks, J. M.; Xu, Q.; Pai, E. F.; Miller, S. M.; Wei, D. Q.; Smith, J. C.; Guo, H.: X-ray Structure of a Hg2+ Complex of Mercuric Reductase (MerA) and Quantum Mechanical/Molecular Mechanical Study of Hg2+ Transfer between the C-Terminal and Buried Catalytic Site Cysteine Pairs. *Biochemistry* **2014**, *53*, 7211-7222.
(47) Khan, M. A. K.; Wang, F. Y.: Mercury-Selenium Compounds And Their Toxicological Significance: Toward A Molecular Understanding Of The Mercury-Selenium Antagonism. *Environ. Toxicol. Chem.* **2009**, *28*, 1567-1577.
(48) Khan, M. A. K.; Asaduzzaman, A. M.; Schreckenbach, G.; Wang, F. Y.: Synthesis, Characterization and Structures of Methylmercury Complexes with Selenoamino Acids. *Dalton Trans.* **2009**, 5766-5772.
(49) Asaduzzaman, A. M.; Khan, M. A. K.; Schreckenbach, G.; Wang, F.: Computational Studies of Structural, Electronic, Spectroscopic and Thermodynamic Properties of Methylmercury-Amino Acid Complexes and their Se Analogues. *Inorg. Chem.* **2010**, *49*, 870-878.
(50) Asaduzzaman, A. M.; Schreckenbach, G.: Degradation Mechanism of Methyl Mercury Selenoamino Acid Complexes: A Computational Study. *Inorg. Chem.* **2011**, *50*, 2366-2372.
(51) Asaduzzaman, A. M.; Schreckenbach, G.: Chalcogenophilicity of Mercury. *Inorg. Chem.* **2011**, *50*, 3791-3798.
(52) Khan, M. A. K.; Wang, F. Y.: Chemical Demethylation of Methylmercury by Selenoamino Acids. *Chem. Res. Toxicol.* **2010**, *23*, 1202-1206.
(53) Smith, R. M.; Martell, A. E.; Motekaitis, R. J.: NIST Standard Reference Database 46. NIST Critically Selected Stability Constants of Metal Complexes Database. Version 2. 2003.
(54) Hammond, G. E.; Lichtner, P. C.; Mills, R. T.: Evaluating the performance of parallel subsurface simulators: An illustrative example with PFLOTRAN. *Water Resour. Res.* **2014**, *50*, 208-228.

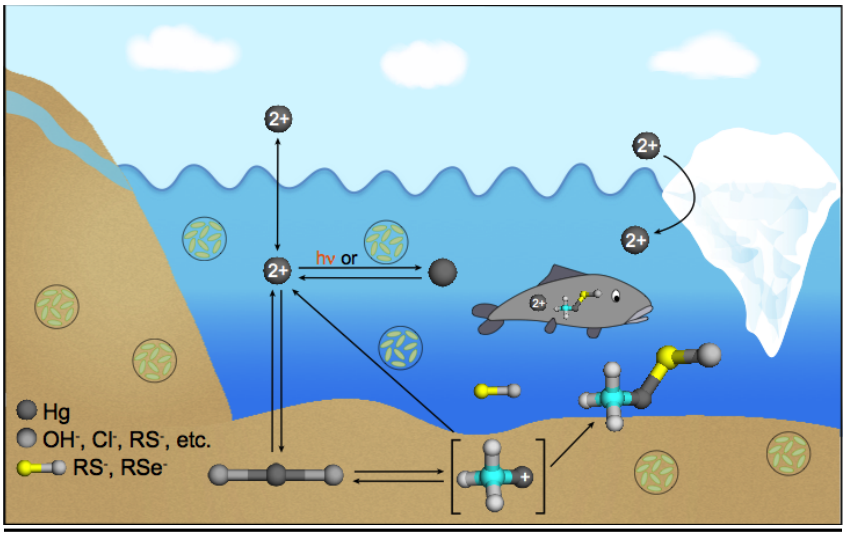
2+
2+
2+
hv or
2+
Hg
OH-, Cl-, RS-, etc.
RS-, RSe-